ORIGINAL ARTICLE

Effect of Different Minority Carrier Lifetime of Multicrystalline Wafer on Solar Cell Performance

Xiaolan Yi*

Tianfu New Area General Aviation Profession Academy, Meishan 620564, China. E-mail: zhangpeng_cd@163.com

Abstract: In thisarticle, a study of the effect of different minority carrier lifetime (τ) of wafers on solar cell performance in a conventional industrial production line has been carried out. The results clearly showed that the ultimate efficiency of the solar cells made by wafers of 1μs <τ<1.2μs and 1.2μs <τ<1.5μs is much higher than that of solar cells made by wafers of τ<1μs. The gap of both is about 0.38%–0.53%. Differently, there is no significant difference between wafers of 1μs<τ<1.2μs and 1.2μs <τ<1.5μs. The results obtained are useful when the solar cell companies establish original wafers test standard in industry.

Keywords: Minority Carrier Lifetime; Multicrystalline Silicon; Cell Performance

1. Introduction

The material of boron-doped multicrystalline silicon is the most relevant material in today's solar cell production. The minority carrier lifetime gives an indication of material quality and suitability for solar cell use. Because of the lattice defect, residual impurities such as carbon oxygen and metal ions, the minority carrier lifetime of multicrystalline silicon wafers is about 1μs. The lifetime of wafer is significantly effect by solar cell fabrication steps, so we tested the minority lifetime of wafers after phosphorus diffusion by a method of quasi steady state photoconductor (QSSPC). The QSSPC is a contactless, highly sensitive, area-averaged lifetime measurement method[1]. It can give similar results to a more sophisticated analysis with high-resolution mapping data. BERGER Single Cell Testing system performs all measurements of photovoltaic characteristics automatically and all data is saved to the system's database. We want to establish the correlation between minority carrier lifetime of wafer and the ultimate efficiency of the solar cell in this study.

2. Experiment

The wafers used in the experiment were made in China. They are P-type multicrystalline silicon wafers; the area of wafers is 156mm ×156mm. All of the wafers are divided into 4 groups as G1 (τ<1) G2 (τ<1) G3 (1<τ<1.2) G4 (1.2<τ<1.5). The production sequence is G1 G2 G3 G4 and all the groups run in the seam line. The process starts with wafer thinning to about 180-200μm followed by texture etch. Then the front-surface field is formed by phosphorus diffusion, resulting in 60-70 Ω /sq front surface filed. After phosphorus glass removal rear side etch and edge isolation the PECVD SiN anti-reflection coating was deposited on front. Subsequently, the back and front contacts was screen-printed. Both contacts were co-fired in an infrared

doi: 10.18686/esta.v7i4.163

conveyor belt furnace. At the end all cells were tested and sorted by BERGER Single Cell Testing System. The minority lifetime of semi-finished cell was tested after phosphorus diffusion by a method of QSSPC. The instrument is the silicon wafer lifetime tester WCT-120 of sinton instruments.

3. Discussion and results

3.1 Comparison of lifetimes after phosphorus diffusion

In **Table 1**, a significant improvement in lifetime from 1μs to 10μs is seen after the phosphorus diffusion[2]. Firstly the improvement is attributed to the removal contaminants and structural defects from the silicon surface after texture etch, secondly the surface passivation with the oxide layer formed during phosphorus diffusion and the phosphorus gettering of impurities present in wafers have contribution[3]. Via statistical analysis powered by JMP software, we can find the lifetime of wafer after phosphorus diffusion shows no significant difference between groups. The **Figure 1** and **Figure 2** show the details.

Table 1. Summary of lifetime after diffusion

	lifetime after diffusion/μs
GroupID	Mean
G1	9.85278
G2	9.40345
G3	10.4421
G4	10.6846

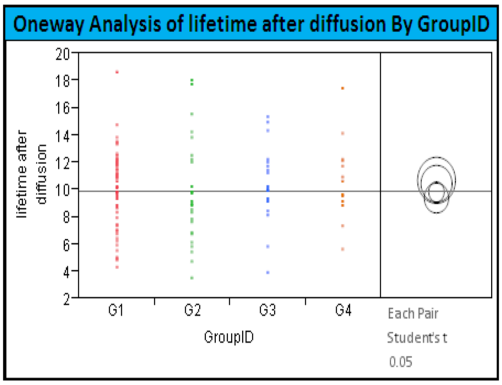

Figure 1. Lifetime after diffusion distribution of each group.

Comparisons for each pair using Student's t

t	Alpha
1.97852	0.05

Abs(Dif)-LSD

	G4	G3	G1	G2
G4	-2.37458	-1.93655	-0.99254	-0.73951
G3	-1.93655	-1.96418	-0.97209	-0.74819
G1	-0.99254	-0.97209	-1.009	-0.88216
G2	-0.73951	-0.74819	-0.88216	-1.58986

Positive values show pairs of means that are significantly different.

Level		Mean
G4	A	10.684615
G3	A	10.442105
G1	A	9.852778
G2	A	9.403448

Levels not connected by same letter are significantly different.

Figure 2. The LSD threshold table shows the difference between the absolute difference in the means and the LSD (least significant different). If the values are positive, the difference in the two means is larger than the LSD, and the two groups are significantly different[4,5].

3.2 Comparison of ultimate efficiency

Table 2 display the mean of Ncell Uoc Isc and FF of each group. The Ncell gap between τ>1μs and τ<1μs is about 0.38%~0.53%. In **Figure 3**, the groups of τ<1 (G1 G2) show significant difference in cell performance compared to the groups of τ>1 (G3 G4) and the group of

1.0<τ<1.2 (G3) shows no significant difference in cell performance compared to the group of 1.2<τ<1.5 (G4). The **Figure 4** shows the distrubution of each group, and the groups of τ>1 (G3 G4) show better distrubution than the groups of τ<1 (G1 G2)[6].

Table 2. Summary of ultimate efficiency

	NCell/%	Uoc/V	Isc/A	FF/%
GroupID	Mean	Mean	Mean	Mean
G1	0.15739	0.6101	8.09022	77.564
G2	0.15858	0.6107	8.11859	77.795
G3	0.16268	0.6153	8.29003	77.599
G4	0.16238	0.6146	8.27585	77.684

Comparisons for all pairs using Tukey-Kramer HSD

q*	Alpha
2.56924	0.05

Abs(Dif)-HSD

	G3	G4	G2	G1
G3	-0.00045	-0.00018	0.00369	0.00493
G4	-0.00018	-0.00051	0.00335	0.00459
G2	0.00369	0.00335	-0.00038	0.00087
G1	0.00493	0.00459	0.00087	-0.00023

Positive values show pairs of means that are significantly different.

Level				Mean
G3	A			0.16268464
G4	A			0.16238370
G2		B		0.15857812
G1			C	0.15739461

Levels not connected by same letter are significantly different.

Figure 3. The Tukey-Kramer HSD threshold matrix shows the actual absolute difference in the means minus the HSD, which is the difference that would be significant. Pairs with a positive value are significantly different.

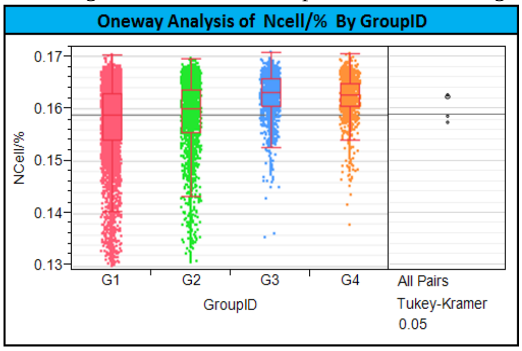

Figure 4. Ncell distrubution of each group.

3.3 Quantum Efficiency (QE) test results

Four cells were tested QE with QEX7. In **Figure 5**, the cell with low Ncell (low τ) has low quantum efficiency especially at long wavelength. The quantum efficiency ideally has a square shape, where the QE value is fairly constant across the entire spectrum of wavelengths measured. However, the QE for most solar cells is reduced because of the effects of recombination, where charge carriers are not able to move into an external circuit. Lower energy (long wavelength) light is absorbed in the bulk of a solar cell, and the wafer of low τ means more recombination. The carriers that the lower energy photons produce must pass through the longer distance to arrive at the PN junction, so the QE of low τ wafers are low at long wavelength[7,8].

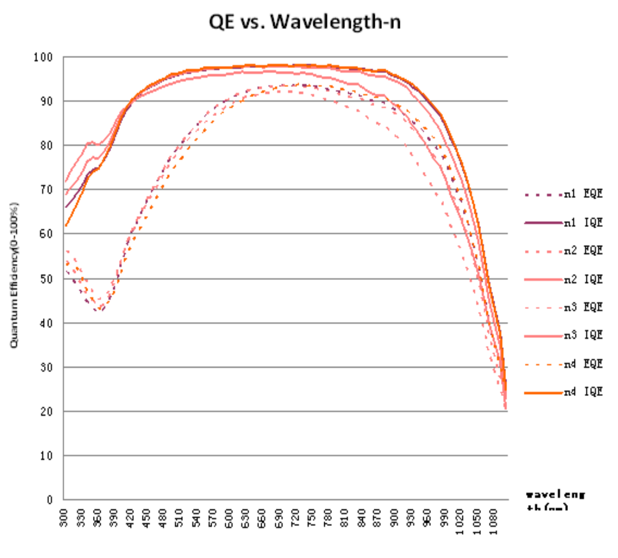

SN	NCell	Uoc	Isc	FF	Rs	Rsh	Irev2
n1	0.16162	0.6176	8.3969	75.838	0.003485	85.884	0.29280
n2	0.15870	0.6128	8.1382	77.432	0.003267	99.189	0.24685
n3	0.15930	0.6136	8.2198	76.851	0.004044	155.214	0.11545
n4	0.16249	0.6215	8.3431	76.257	0.003224	92.858	0.18499

Figure 5. QE test results of cells.

4. Conclusions

The lifetime of wafer after phosphorus diffusion shows no significant difference between groups, but the ultimate efficiency of the solar cell made by wafers of 1μs <τ<1.2μs and 1.2μs <τ<1.5μs is much higher than that of solar cell made by wafers of τ<1μs.

References

1. Khadka DB, Shirai Y, Yanagida M, *et al*. Ammoniated aqueous precursor ink processed copper iodide as hole transport layer for inverted planar perovskite solar cells. Solar Energy Materials & Solar Cells 2020; 210: 110486.
2. Duan Q, Ji J, Hong X, *et al*. Design of hole-transport-material free $CH_3NH_3PbI_3/CsSnI_3$ all-perovskite heterojunction efficient solar cells by device simulation. Solar Energy 2020; 201: 555–560.
3. Elseman AM, Selim MS, Luo L, *et al*. Efficient and stable planar n-i-p perovskite solar cells with negligible hysteresis via solution processed Cu_2O nanocubes as low-cost hole-transport material. ChemSusChem 2019; 12(16): 3808–3816.
4. Liu C, Zhou X, Chen S, *et al*. Hydrophobic Cu_2O quantum dots enabled by surfactant modification as top hole-transport materials for efficient perovskite solar cells. Advanced Science 2019; 6(7): 1801169.
5. Wu X, Xie L, Lin K, *et al*. Efficient and stable carbon-based perovskite solar cells enabled by the inorganic interface of CuSCN and carbon nanotubes. Journal of Materials Chemistry A 2019; 7(19): 12236–12243.
6. Bothe K, Sinton R, Schmidt J. Fundamental boron–oxygen-related carrier lifetime limit in mono- and multicrystalline silicon. Progress in Photovoltaics: Research and Applications 2005; 13(4): 287–296.
7. Sinton RA, Cuevas A, Stuckings M. Quasi-steady-state photoconductance, a new method for solar cell material and device characterization. Conference Record of the Twenty Fifth IEEE Photovoltaic Specialists Conference 1996; 457–460.
8. Dhungela SK, Yooa J, Kima K, *et al*. Study of process induced variation in the minority carrier lifetime of silicon during solar cells fabrication. Materials Science and Engineering: B 2006; 134(2-3): 287–290.